JOURNAL OF MATERIALS SCIENCE 33 (1998) 3699–3710

Two-dimensional charge-transfer molecules for second-order non-linear optics: synthesis, characterization and second harmonic generation of *N,N′*-dialkyl-2,4-dinitro-1,5-diaminobenzene compounds

H. S. NALWA*
Hitachi Research Laboratory, Hitachi Ltd., 7-1-1 Ohmika-cho, Hitachi City, Ibaraki 319-1292, Japan
E-mail: nalwa@hrl.hitachi.co.jp

T. WATANABE, K. OGINO, H. SATO, S. MIYATA
Department of Materials Systems Engineering, Faculty of Technology, Tokyo University of Agriculture and Technology, Koganei, Tokyo 184, Japan

Two-dimensional charge-transfer molecules based on *N,N′*-dialkyl-2,4-dinitro-1,5-diaminobenzene have been synthesized. ^{1}H and ^{13}C-NMR spectroscopy, elemental analysis and mass spectroscopy were used to elucidate their chemical structures. The physical and non-linear optical properties of this new family of dyes containing alkyl chain; C_3H_7, C_6H_{13}, C_8H_{17}, $C_{10}H_{21}$, $C_{11}H_{23}$ and $C_{18}H_{37}$ are discussed, taking into account the possible role of alkyl chain length. These two-dimensional molecules have a significantly large off-diagonal β component in contrast to one-dimensional molecules. These compounds showed no powder second-harmonic generation (SHG) at 1.064 μm being centrosymmetric, however, their poled guest-host systems with poly(methyl methacrylate) and co-crystals with *p*-nitroaniline were SHG active. Powder SHG as high as 37 times that of urea was observed from *N,N′*-dihexyl-2,4-dinitro-1,5-diaminobenzene with its mixture with *p*-nitroaniline. Second-harmonic generation of *N,N′*-dioctadecyl-2,4-dinitro-1,5-diaminobenzene (DIODD) was studied as Langmuir–Boldgett monolayers. The Langmiur–Blodgett monolayer of a 1:1 mixture of DIODD and arachidic acid showed second-order non-linear optical coefficients d_{11} and d_{13} of 11×10^{-9} and 3.85×10^{-9} esu, respectively, at a tilt angle of 60°. For the first time, a relationship between the microscopic polarizabilities and the molecular orientation of two-dimensional charge-transfer molecules has been established. In the light of the present experimental and theoretical data analysis, the potential of two-dimensional charge-transfer molecules for second-order non-linear optics is discussed. © *1998 Kluwer Academic Publishers*

1. Introduction

Organic non-linear optical materials are of considerable interest because of their potential applications in second- and third-order non-linear optics that include harmonic generation, electro-optical modulators, memory, optical switches, interconnects, and other photonic devices [1–9]. From the symmetry point of view, it is known that a necessary criterion for a material to exhibit second-harmonic generation is that it must lack a centre of symmetry. Unfortunately, the majority of organic molecules crystallize in centrosymmetric space groups. To introduce non-centrosymmetry, a number of strategies such as hydrogen bonding, steric hindrance, chirality, electrical poling, dye–polymer blending, co-crystallization, lambda (Λ)-type molecules, organometallic structures, etc., have been proposed [4, 5, 10, 11]. Another important tool for inducing SHG activity is the Langmuir–Boldgett (LB) technique, as it underlies most of the functions in forming acentric structure. In this connection, the molecular architecture of organic species provides the basis of new non-linear optical materials. In organic materials, second-order non-linear optical effects originate from a π-electron conjugated system consisting of electron acceptor and electron donor functionalities. The derivatives of *p*-nitroaniline represent such a model system. We have designed and developed a series of *N,N′*-dialkyl-2,4-dinitro-1,5-diaminobenzenes.

*Author to whom all correspondence should be addressed.

0022–2461 © *1998 Kluwer Academic Publishers*

These derivatives have a two-dimensional charge transfer (2-D CT) structure, contrary to *p*-nitroaniline which is a one-dimensional charge-transfer (1-D CT) molecule. These two-dimensional charge-transfer molecules also possess the large hyperpolarizabilities. Previous studies on the SHG properties have been focused mainly to classical one-dimensional charge-transfer molecules, either in their bulk state or Langmuir–Blodgett films that include merocyanines, azobenzenes, amidonitrostilbenes, phenylhydrazone dyes, styrylpyridinium salts, diazostilbenes, and polyenes [12–17]. We for the first time addressed that two-dimensional charge-transfer molecules so being equally important for second-order non-linear optics. One of the interesting features of two-dimensional charge-transfer molecules is that their off-diagonal β component (β_{xyy}) is several-fold larger than the diagonal components [18, 19]. If we consider the case of LB films of one-dimensional charge-transfer molecules, they exhibit optimum second-harmonic generation efficiency when the LB molecules are aligned normal to the substrate. However, the LB molecules having bulky alkyl groups, inherently tend to incline from normal to the substrate causing the magnitude of optical non-linearities to decrease from the optimum values. In order to overcome this problem, we have developed a series of two-dimensional charge-transfer dyes that exhibit large SHG from LB monolayers even though the LB molecules are inclined from normal to the substrate. It has been demonstrated that SHG activity of poled polymers can be stabilized when two-dimensional charge-transfer molecules are utilized, because they behave very differently than those of one-dimensional charge-transfer molecules. Our theoretical and experimental studies show that two-dimensional charge-transfer molecules have a great potential for frequency doubling.

In this paper, we report the chemical synthesis and analytical characterization of *N*,*N*′-dialkyl-2,4-dinitro-1,5-diaminobenzenes. The influence of alkyl chain length (C_nH_{2n+1} where *n* is 3, 6, 8, 10, 11 and 18) on the physical properties is discussed. The results of ^{1}H and ^{13}C-NMR spectroscopic studies of *N*,*N*′-dialkyl-2,4-dinitro-1,5-diaminobenzenes are presented. These two-dimensional charge-transfer molecules show no SHG in bulk state, however, their guest-host systems with poly(methyl methacrylate) PMMA and *p*-nitroaniline are SHG active. Guest-host systems of two-dimensional charge-transfer molecules with PMMA exhibit SHG in the poled state, while instantaneous SHG is observed from *p*-nitroaniline mixtures without applying any electric poling. We have earlier described the theoretical modelling of the two-dimensional charge-transfer molecules and poled PMMA films. Interestingly, we have found that two-dimensional charge-transfer molecule *N*,*N*′-dioctadecyl-2,4-dinitro-1,5-diaminobenzenes (DIODD) shows large SHG in Langmuir–Boldgett monolayers. For the first time, a relationship between the microscopic polarizabilities and molecular orientation of two-dimensional charge-transfer molecules is reported to add a new direction to the molecular designing of LB films for SHG. Furthermore, the first hyperpolarizability (β) calculations performed as a function of the tilt angle demonstrated that the second-order optical non-linearity in two-dimensional charge-transfer molecules is optimized when the molecule is inclined at a tilt angle of 56° from normal to the substrate, unlike one-dimensional charge-transfer molecules.

2. Experimental procedure

2.1. Synthesis

N,*N*′-Dialkyl-2,4-dinitro-1,5-diaminobenzenes were synthesized by the following method (synthesis Scheme I). In first step, 1,5-dihalo-2,4-dinitrobenzenes were obtained by the nitration (HNO_3/H_2SO_4) of *meta*-dihalobenzene. In the second step, *N*,*N*′-dialkyl-2,4-dinitro-1,5-diaminobenzenes were prepared by an elimination–substitution reaction of 1,5-dihalo-2,4-dinitrobenzenes with corresponding alkylamines. 2,4-Dinitro-1,5-diaminobenzene was obtained in a two-step reaction: first nitration of *m*-difluorobenzene gives 1,5-difluoro-2,4-dinitrobenzene and secondly, the final product 2,4-dinitro-1,5-diaminobenzene was obtained by passing ammonia gas through an ethylene glycol solution of 1,5-difluoro-2,4-dinitrobenzene. The derivatives containing alkyl chains of propyl (C_3H_7), hexyl (C_6H_{13}) and octyl (C_8H_{17}) were obtained in ethylene glycol; alkyl chain of decyl ($C_{10}H_{21}$) and undecyl ($C_{11}H_{23}$) in *N*,*N*′-dimethylformamide (DMF) and alkyl chain of octadecyl ($C_{18}H_{37}$) also in DMF using Na_2CO_3 as a catalyst. The reaction temperature was maintained between 120 and 140 °C for a period of about 20 h. All of these materials were purified by column chromatography using silica gel as a stationary phase and chloroform/hexane (3/1) eluent followed by recrystallization in absolute methanol. The yield depends on an individual reaction and generally can be counted in the range of 40%–75%.

2.2. Spectroscopic characterization

The melting points of the compounds were determined by differential scanning calorimetery (DSC) technique at a heating rate of 20 °C min^{-1} on a Rikagu system (model TGA-DSC CN8085El, Rikagu Denki Co. Japan). The molecular weight of the compounds was measured by ionized method using a Jeol mass spectrometer (model JMS-HX100/JMA-DA5000). ^{1}H and ^{13}C-NMR spectra were recorded at room temperature (ca. 30 °C) by a Jeol GX-270

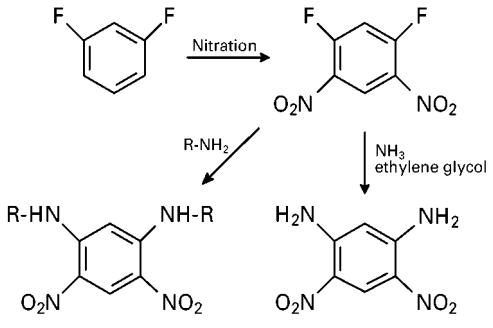

Scheme I

nuclear magnetic resonance spectrometer (270 MHz for ^{1}H and 67.5 MHz for ^{13}C). The selective decoupling experiments were performed on a Jeol FX-200 spectrometer (200 MHz for ^{1}H and 50 MHz for ^{13}C). For ^{1}H and ^{13}C-NMR measurements, the concentrations of the samples were approximately 5% and 20% by weight (wt/vol) in deuteriochlorofom ($CDCl_3$), respectively. In the case of ^{1}H NMR, the chemical shifts were calibrated in reference to tetramethylsilane (TMS; 0.0 p.p.m.) whereas for ^{13}C-NMR, calibration was done from deuteriochloroform by converting them to a TMS scale ($CDCl_3$; 77.0 p.p.m.).

2.3. Second-order NLO measurements

To establish a structure–property relationship, the first hyperpolarizabilities of a variety of two-dimensional charge-transfer model compounds were calculated according to the finite field method using the Molecular Orbital Package (MOPAC) AM1 [20]. A Nd–YAG Q-switched laser operating at a 1.064 μm fundamental wavelength with a pulse of 10 ns and a repetition rate of 10 Hz was used for the powder SHG and second-order non-linear susceptibility $\chi^{(2)}(-2\omega; \omega, \omega)$ measurements. The LB films deposited on both sides of the substrate were illuminated and light was transmitted on the other side. The fundamental beam was filtered by an infrared cut-filter. The resulting *p*-polarized second-harmonic intensities were measured over a range of angle of incidence ($\pm 60^{\circ}$) and were detected with a photomultiplier. The refractive index of the LB films was measured on Y-type multilayers (14 layers) deposited on a naturally oxidized silicon substrate by the ellipsometry technique using argon and He–Ne lasers.

3. Results and discussion

3.1. Materials characterization

Table I lists the physical properties of *N*,*N*′-dialkyl-2,4-dinitro-1,5-diaminobenzenes. The elemental analysis data of all the compounds are in good agreement with the calculated ones. The molecular weights obtained by the ionized method using mass spectroscopy were in excellent agreement with the formula weights. 2,4-dinitro-1,5-difluorobenzene and 2,4-dinitro-1,5-dichlorobenzene have melting points of 82–83 and 103–105 °C, respectively. 2,4-Dinitro-1,5-diaminobenzene which has no alkyl chain, shows a melting point of about 298 °C due to the strong hydrogen bonding between amino and nitro groups (Fig. 1). The melting point decreases to 155 °C for an alkyl chain of C_3H_7 because the substitution of the alkyl chain breaks the hydrogen bonding which lowers the thermal stability. Later the melting point is dependent on alkyl chain length and it increases as the alkyl chain increases. Presumably, this behaviour originates from the crystallization of alkyl chains. These compounds exhibit absorption maxima in the range of 410–420 nm and have a cut-off wavelength of about 470 nm.

Fig. 2 shows the ^{1}H-NMR spectrum of *N*,*N*′-dihexyl-2,4-dinitro-1,5-diaminobenzene recorded in deuteriochloroform. The proton assignment is depicted on the spectrum. The aromatic proton on C_6 appears at 5.69 p.p.m., while one on C_3 appears at 9.29 p.p.m. The amino protons are located at 8.37 p.p.m. The α, β and γ methylene protons of the alkyl group appear at 3.32, 1.85 and 1.52 p.p.m. respectively. All other methylene protons (4 protons) are centred at 1.43 p.p.m. The terminal methyl protons occur at 0.97 p.p.m. The ^{1}H-NMR spectrum supports the chemical structures of *N*,*N*′-dihexyl-4,6-dinitro-1,5-diaminobenzene. The chemical shifts of other compounds are listed in Table II and the quantitative results are in excellent agreement. We also found that if one of the aminoalkyl chains is replaced by a halogen such as fluorine or chlorine, the chemical shifts are significantly affected. In particular, an aromatic proton on C_6(Hb) has a significant effect. For example, the Hb proton of *N*-decyl-2,4-dinitro-5-chloroaminobenzene

TABLE I Elemental analysis, molecular weights and melting points of *N*,*N*′-dialkyl-2,4-dinitro-1,5-diaminobenzenes

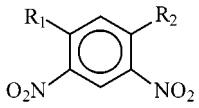

$R_1 = R_2$	Elemental analysis					Molecular weight	Melting point (°C)
		C (%)	N (%)	H (%)	C (%)		
NH_2	Found	33.80	21.26	1.98	30.68	198	298–300
	Calc.	36.36	28.28	3.03	32.32		
$NH–(CH_2)_2–CH_3$	Found	50.53	19.64	6.56	22.15	282	153–155
	Calc.	51.06	19.85	6.40	22.69		
$NH–(CH_2)_5–CH_3$	Found	58.55	15.17	8.34	18.21	367	57–58
	Calc.	59.01	15.30	8.29	17.48		
$NH–(CH_2)_7–CH_3$	Found	61.72	13.03	9.22	16.11	423	83–84
	Calc.	62.55	13.27	9.00	15.169		
$NH–(CH_2)_9–CH_3$	Found	64.96	11.60	10.00	14.10	479	88–89
	Calc.	65.26	11.71	9.62	13.38		
$NH–(CH_2)_{10}–CH_3$	Found	64.14	10.80	9.69	13.33	507	91–92
	Calc.	66.40	11.06	9.88	12.65		
$NH–(CH_2)_{17}–CH_3$	Found	71.11	7.92	11.19	10.46	703	105–107
	Calc.	71.17	7.97	11.11	9.11		

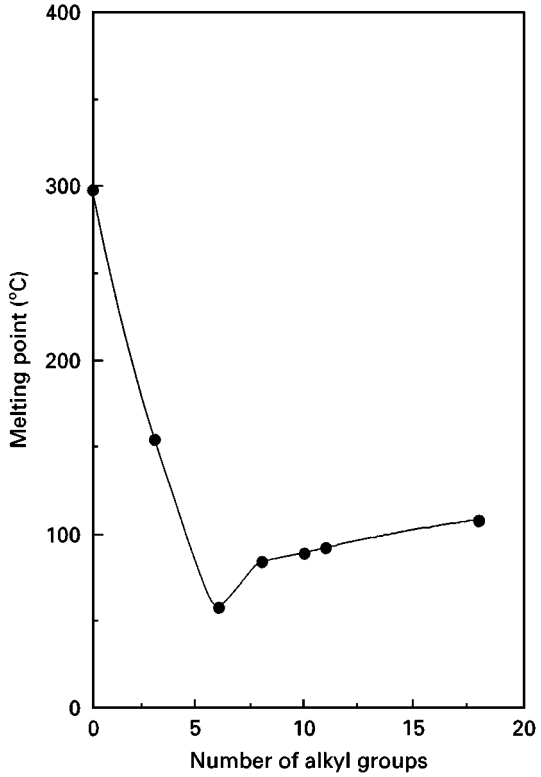

Figure 1 Melting-point dependence on the alkyl chain length for DADB derivatives.

TABLE II ^{1}H-NMR chemical shifts of *N*,*N*′-dialkyl-2,4-dinitro-1,5-diaminobenzenes

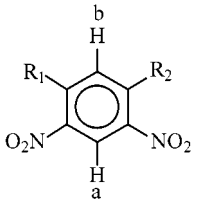

$R_1 = R_2$ = NH–CH_2–CH_2–CH_2–$(CH_2)_n$–CH_3 (c d e f g–h i)

Alkyl chain length	Proton assignment							
	a	b	c	d	e	f	g–h	i
C_3H_7	9.25	5.675	8.362	3.317	1.862			1.156
C_6H_{13}	9.292	5.694	8.378	3.319	1.855	1.539	1.415	0.970
C_8H_{17}	9.286	5.682	8.368	3.315	1.840	1.502	1.359	0.931
$C_{10}H_{21}$	9.226	5.622	8.306	3.315	1.761	1.458	1.256	0.880
$C_{11}H_{23}$	9.218	5.618	8.302	3.309	1.777	1.473	1.249	0.878
$C_{18}H_{37}$	9.298	5.694	8.382	3.317	1.818	1.477	1.312	0.934
$R_1 = Cl$ $R_2 = C_{10}H_{21}$	9.198	6.565	8.501	3.315	1.752	1.452	1.295	0.898

appears at 6.56 p.p.m. while that of *N*,*N*′-didecyl-2,4-dinitro-1,5-diaminobenzene appears at 5.62 p.p.m.

Fig. 3 shows the ^{13}C-NMR spectrum of *N*,*N*′-dihexyl-2,4-dinitro-1,5-diaminobenzene. The carbon assignments were obtained by empirical calculations as well as by the selective decoupling experiments. For the assignment of aromatic carbons, a rough estimation from the empirical formula was derived by a method already reported in the literature [21]. For calculating ^{13}C chemical shifts of the alkyl chain, first the chemical shifts were determined by the Lindeman and Adams equation [22] and then a substituents effect was added by the method of Savitsky and Namikawa [23]. The calculated chemical shifts are

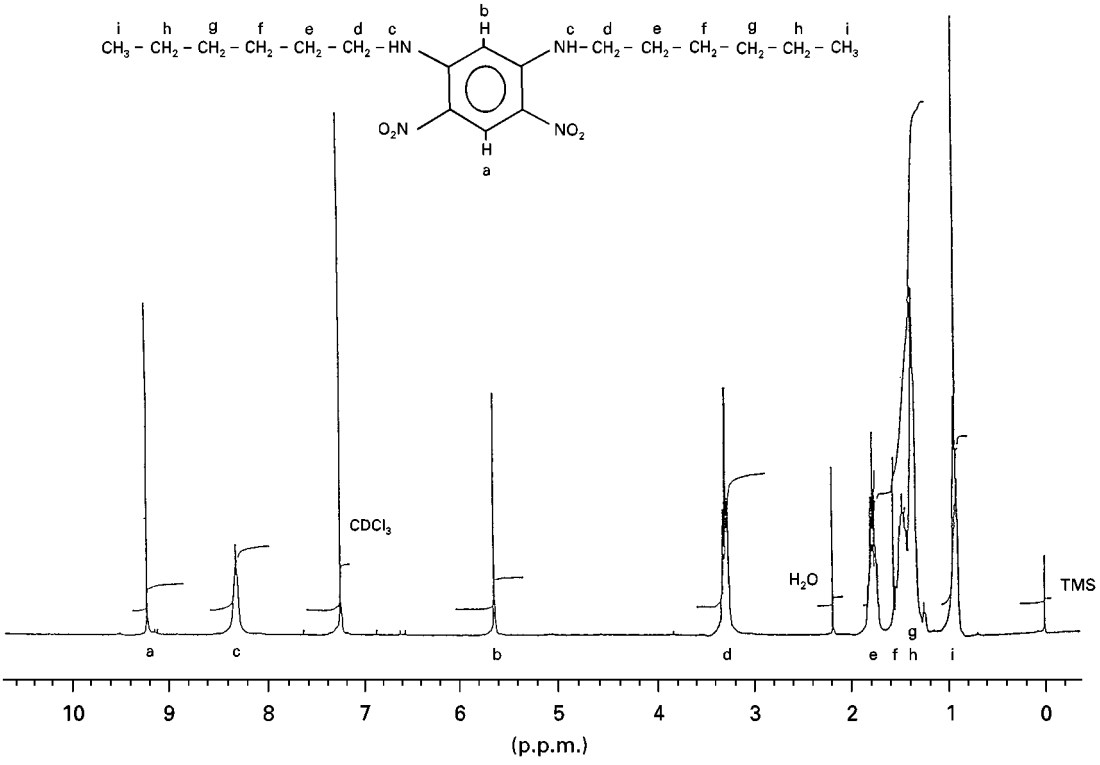

Figure 2 ^{1}H-NMR spectrum of *N*,*N*-dihexyl-2,4-dinitro-1,5-diaminobenzene recoded in deuteriochloroform at room temperature.

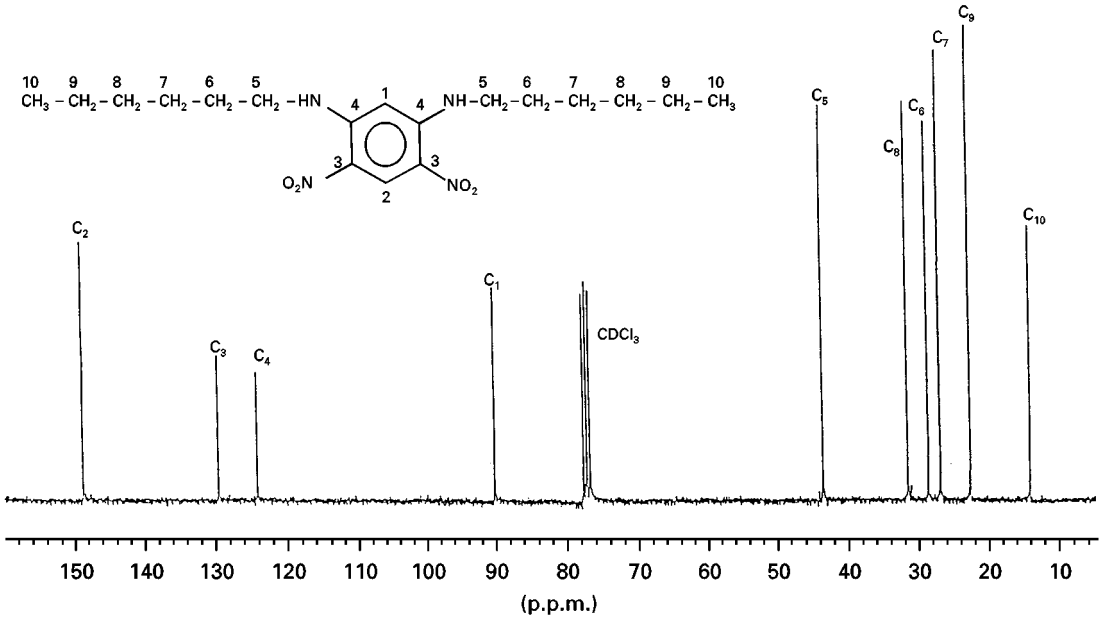

Figure 3 ^{13}C-NMR spectrum of *N*,*N*′-dihexyl-2,4-dinitro-1,5-diaminobenzene recoded in deuteriochloroform at room temperature.

TABLE III ^{13}C-NMR chemical shifts of *N*,*N*′-dihexyl-2,4,-dinitro-1,5-diaminobenzene obtained by experimental analysis and calculated empirically[a,b,c]

Carbon atom	Experimental values	Calculated values
C_1	103.70	90.018
C_2	148.40	148.570
C_3	126.30	129.425
C_4	122.70	123.985
C_5	53.36	48.353
C_6	30.25	28.409
C_7	27.95	26.729
C_8	32.15	31.389
C_9	22.65	22.481
C_{10}	13.86	13.909

[a]Chemical shifts of benzene carbon atoms were calculated using a method reported in the literature.
[b]Chemical shifts of alkyl chain carbons were evaluated using Lindeman and Adams' equation.
[c]The adding substituent effect by Satitsky and Namikawa's parameter.

within the scatter of experimental error (Table III). The signal assignment of the alkyl chain was confirmed by selective decoupling measurements. The signals of methyl, methylene next to methyl (C_{10}), and α-methylene (C_α) carbons are easily separable, because they have different chemical shifts from the others. The signals of C_β, C_γ and C_δ were determined by the selective decoupling technique. By decoupling protons located at 1.85, 1.52 and 1.43 p.p.m., signals at 30.25, 27.95, 32.15 and 22.65 p.p.m., respectively become stronger than other carbons. Therefore, signals at 30.25 p.p.m. can be assigned to C_β and 27.95 p.p.m. to C_γ. The carbons at 32.15 and 22.65 p.p.m. have connectivity to protons located at 1.43 p.p.m. The signal at 32.15 p.p.m. can be assigned to C_δ, hence the signal at 22.65 p.p.m. is attributed to C_ε. Table IV lists the carbon chemical shifts obtained experimentally for

TABLE IV ^{13}C-NMR chemical shifts of *N*,*N*′-dialkyl-2,4,-dinitro-1,5-diaminobenzene compounds

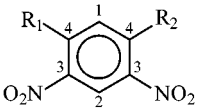

R = –CH_2–CH_2–CH_2–$(CH_2)_n$–CH_2–CH_2–CH_3 (5 6 7 *n* 8 9 10)

Carbon no	$R_1 = R_2 =$ NHR					
	C_3H_7	C_6H_{13}	C_8H_{17}	$C_{10}H_{21}$	$C_{11}H_{23}$	$C_{18}H_{37}$
C_1	90.09	90.01	90.00	90.00	90.18	90.29
C_2	148.61	148.57	148.49	148.52	148.70	148.83
C_3	129.50	129.42	129.24	129.34	129.42	129.50
C_4	124.00	123.98	123.89	123.93	124.18	124.33
C_5	45.08	43.35	43.35	43.33	43.41	43.47
C_6	21.80	28.40	28.45	28.44	28.56	28.65
C_7	11.60	26.72	27.06	27.06	27.11	27.17
C_n			29.20	29.25	29.29	29.32
			29.11	29.47	29.49	29.37
					29.55	29.54
					29.58	29.60
						29.72
C_8		31.38	31.72	31.83	31.89	31.97
C_9		22.48	22.58	22.61	22.64	22.69
C_{10}		13.90	14.01	14.03	14.00	14.01

N,*N*′-dialkyl-4,6-dinitro-1,3-diaminobenzenes containing alkyl chains of C_3H_7, C_6H_{13}, C_8H_{17}, $C_{10}H_{21}$, $C_{11}H_{23}$, and $C_{18}H_{37}$. The chemical shifts are in good agreement and the assignments of carbons have been followed from *N*,*N*′-dihexyl-2,4-dinitro-1,5-diaminobenzene. We have successfully assigned carbons up to alkyl chain length C_6H_{13}. As the alkyl chain increases, the overlapping of peaks takes place which hinders location of the exact position. Only six carbons of alkyl chains ranging C_6H_{13} and $C_{18}H_{37}$ are easily detectable because their chemical shifts lie

in a very close proximity. On the other hand, it is also possible to isolate carbon signals of alkyl chain length $C_{10}H_{21}$, in *N*-alkyl-2,4-dinitro-3-chloroaminobenzene. In disubstituted derivatives, the introduction of an alkyl chain at C_3 makes it difficult to separate carbons beyond C_8H_{17}.

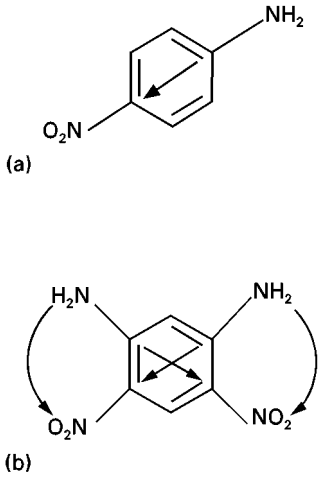

Figure 4 Charge-transfer interactions in (a) One- and (b) two-dimensional systems. (a) 4-nitroaniline (*p*-NA) (b) 1,5-diamino-2,4-dinitrobenzene.

3.2. Second-order non-linear optical properties

Table V lists the β values of two-dimensional charge-transfer molecules calculated by using the MOPAC-AM1 method. Fig. 4 shows the charge-transfer interactions for one-dimensional molecules *p*-NA and two-dimensional molecule 2,4-dinitro-1,5-diaminobenzene. The *p*-NA has one charge-transfer pathway. The latter has amino groups located at *para* as well as *ortho*-positions to the nitro groups, therefore dominantly *para* and *quasi-ortho* interactions lead to a two-dimensional charge-transfer character. It has four charge-transfer pathways. Theoretical calculations demonstrated that the largest β component for 2,4-dinitro-1,5-diaminobenzene is β_{xyy} whilst β_{xxx} is the largest for the *p*-NA molecule. The main difference in β tensors arises from the large off-diagonal components for 2,4-dinitro-1,5-diaminobenzene to the β_{xxx} for *p*-NA. The β components of other two-dimensional charge-transfer materials; 1,5-difluoro-2,4-dinitrobenzene,1,5-dichloro-2,4-dinitrobenzene, *N*,*N*′-dimethyl-2,4-dinitro-1,5-diaminobenzene, and *N*,*N*′-diethyl-2,4-dinitro-1,5-diaminobenzene can be compared. It is apparent that the replacement of halogens by amino groups causes a change in the sign of β as well as a significant increment in β value due to a two-dimensional charge-transfer interaction. Furthermore, the β increases with increasing the length of the alkyl hydrocarbon chain; however, numerical data given here for only methyl and ethyl substituents showed a modest difference. In an other study, we observed that for *N*-alkyl-2,4-dinitro-5-fluoroanilines, the β value increases with increasing alkyl chain length [24]. For example, the β value of *N*-methyl-2,4-dinitro-5-fluoroaniline was found to be about two-fold larger than that of *N*-propyl-2,4-dinitro-5-fluoroaniline. *N*,*N*′-diethyl-2,4-dinitro-1,5-diaminobenzene shows a β value of 10.64×10^{-30} esu, slightly smaller than the *p*-NA molecule. The magnitude of the

TABLE V Polarizabilities, hyperpolarizabilities and dipole moments (μ) of model compounds 1,5-difluoro-2,5-dinitrobenzene, 1,5-dichloro-2,4-dinitrobenzene, *N*,*N*′-dimethyl-2,4-dinitro-1,5-diaminobenzene, and *N*,*N*′-diethyl-2,4-dinitro-1,5-diaminobenzene calculated by using the MOPAC-AM1 method [20]. The dialkyl derivatives of DADB are representative of the two-dimensional charge-transfer molecules. The electron-donating amino or alkylamino groups are located at *para* as well as *ortho*-positions to the electron-accepting nitro groups, therefore dominantly *para* and *quasi-ortho* interactions lead to a two-dimensional charge-transfer character. The orientationally averaged hyperpolarizability is given by $\beta_x = \beta_{xxx} + \beta_{xyy} + \beta_{xzz}$

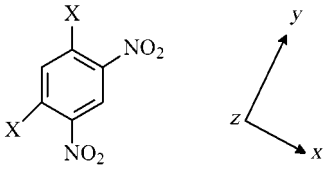

β components	Molecular hyperpolarizability (10^{-30} esu)				
	X = Cl	X = F	X = NH_2	X = NH–CH_3	X = NH–CH_2–CH_3
β_{xxx}	1.036	1.937	− 3.114	− 3.096	− 2.792
β_{xyy}	− 4.556	9.873	9.873	12.195	13.640
β_{xzz}	− 0.180	− 0.125	0.034	0.230	− 0.206
β_{yyy}	− 0.491	− 0.300	0.327	0.461	0.367
β_{yxx}	− 0.060	0.014	− 0.038	− 0.101	− 0.101
β_{yzz}	− 0.063	0.008	− 0.019	0.002	− 0.118
β_{zzz}	− 0.007	− 0.011	0.009	− 0.014	− 0.050
β_{zxx}	0.034	0.014	− 0.031	0.002	0.007
β_{zyy}	0.028	0.017	− 0.620	− 0.015	− 0.034
β_x	− 3.70	− 1.69	6.793	8.869	10.642
α (10^{-23} esu)	2.896	2.543	3.071	3.646	4.108
γ (10^{-36} esu)	6.825	0.077	29.71		19.53
μ (Debye)	4.777	3.956	7.36	7.878	8.253

β value of two-dimensional molecules is the same as of *p*-NA [25, 26]. 2,4-Dinitro-1,5-diaminobenzene analogues are particularly important from the viewpoint of their large off-diagonal β_{xyy} component which is three to five times larger than that of the diagonal β_{xxx} component. For other two-dimensional charge-transfer molecules such as MANN, β_{xyy} as large as 32 times that of the β_{xxx} component has been observed. Interestingly the ratio between β_{xyy} and β_{xxx} components grows to 396 for the OANN molecule [27]. From the same calculations, β_{xxx} is six times that of the β_{xyy} component for the *p*-NA molecule, respectively, because of its one-dimensional charge-transfer character. Cheng *et al.* [25] reported a β value of 9.2×10^{-30} esu and Kondo *et al.* [26] a value of 12.6×10^{-30} esu for *p*-NA. The β values of two-dimensional charge-transfer molecules with shorter alkyl chain are of the same magnitude.

The substitution of the alkyl chain contributes to increasing the electron donating activity of amino groups. Furthermore, as the alkyl chain length increases up to $C_{18}H_{37}$, it facilitates in developing Langmuir–Blodgett monolayers on the water subphase. All of these compounds except *N*,*N*′-dioctyl-2,4-dinitro-1,5-diaminobenzene crystallize in centrosymmetric space groups because they exhibit no powder SHG activity. *N*,*N*′-dioctyl-2,4-dinitro-1,5-diaminobenzene shows very weak powder SHG activity in the bulk state. This compound posseses polymorphism, because its SHG activity disappears after sometime, presumably due to the transformation to another phase which makes it SHG inactive. Table VI lists the melting points and powder SHG activity of 17 different materials based on *N*-alkyl-2,4-dinitro-5-fluoroanilines and *N*,*N*′-dialkyl-2,4-dinitro-1,5-diaminobenzenes when mixed with *p*-NA in a 1 : 3 ratio (dye: *p*-NA). The mixed crystals of these compounds with *p*-NA were prepared either in chloroform or acetone. SHG activity of these *p*-NA mixed compounds are low and only compound 13 shows powder SHG of 37 times that of urea for 1.01 mixture. Compounds 4 and 14 show powder SHG of 2.0 and 2.26 times that of urea. As can be seen, SHG activity also depends upon the dye–*p*-NA ratio, for example, the SHG activities of compound 14 are 2.26, 2.65, 20.8 and 0.03 times larger than that of urea for 1 : 4, 1 : 3, 1 : 0.1 and 1 : 10 ratios, respectively. For compound 13, the powder SHG changes by more than an order of magnitude. A simple factor that contributes to the difference in SHG activity may be the effect of crystallite size which has a profound effect on powder SHG measurements. SHG activity originates from the co-crystallization of two-dimensional molecules with *p*-NA which introduces a non-centrosymmetric structure. Okamoto *et al.* [28, 29] reported very large powder SHG for the composites of *p*-NA and its *N*-alkyl derivatives. For example, the mixtures of *p*-NA with *N*-isopropyl-4-nitroaniline in a weight ratio of 0 : 1, 1 : 1, 1 : 0.1, 1 : 0.2 and 1 : 0.5 showed powder SHG of 1.5, 250, 163, 280 and 416 times larger than that of urea, respectively. Our studies on a 2 : 1 mixture of *N*-9-octadecenyl-4-nitroaniline to *p*-NA also showed a powder SHG of 135 times larger than urea. Our results also support that the co-crystallization of two-dimensional charge-transfer molecules with *p*-NA is another avenue for introducing SHG activity. SHG coefficient of

TABLE VI A series of alkyl derivatives of 2,5-dinitrobenzene and their powder SHG from a *p*-nitroaniline mixture (dye: *p*-NA 1 : 3 ratio)

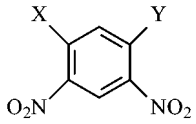

No	X	Y	Melting point (°C)	SHG (*x* Urea)
1	F	F	82–83	–
2	Cl	Cl	103–105	–
3	NH_2	NH_2	298–300	
4	Cl	$NH–(CH_2)_9–CH_3$	57–59	2.0
5	Cl	$NH–(CH_2)_{11}–CH_3$	66–68	1.7
6	F	$NH–(CH_2)_{12}–CH_3$	59–60	0.15
7	F	$NH–(CH_2)_{15}–CH_3$	63–64	0.10
8	F	$NH–(CH_2)_{17}–CH_3$	64–66	0.02
9	Cl	$NH–(CH_2)_{17}–CH_3$	67–69	0.02
10	$NH–CH_3$	$NH–CH_3$	–	–
11	$NH–CH_2–CH_3$	$NH–CH_2–CH_3$	–	–
12	$NH–(CH_2)_2–CH_3$	$NH–(CH_2)_2–CH_3$	153–155	0.03
13	$NH–(CH_2)_5–CH_3$	$NH–(CH_2)_5–CH_3$	58–60	0.8 36.78 (1 : 0.1) 0.16 (1 : 10)
14	$NH–(CH_2)_7–CH_3$	$NH–(CH_2)_7–CH_3$	84–86	2.26 (1 : 4) 2.65 (1 : 3) 20.8 (1 : 0.1) 0.03 (1 : 10)
15	$NH–(CH_2)_9–CH_3$	$NH–(CH_2)_9–CH_3$	89–90	0.02
16	$NH–(CH_2)_{10}–CH_3$	$NH–(CH_2)_{10}–CH_3$	91–92	0.00
17	$NH–(CH_2)_{17}–CH_3$	$NH–(CH_2)_{17}–CH_3$	106–107	0.43

TABLE VII Refractive indices and NLO coefficients of dyes dispersed in a PMMA matrix

Compound no.	Dye weight (%) in PMMA	Refractive indexes		NLO coefficients ($pm\,V^{-1}$)
		0.523 μm	1.064 μm	
4	16.62	1.53	1.484	$d_{33} = 2.7$ $d_{31} = 0.88$
6	16.32	1.507	1.497	$d_{33} = 2.64$ $d_{31} = 0.70$
7	15.61	1.51	1.49	$d_{33} = 1.80$ $d_{31} = 0.84$
12	16.66	1.498	1.488	$d_{33} = 2.4$ $d_{31} = 0.31$
13	16.62	1.513	1.482	$d_{33} = 3.78$ $d_{31} = 1.12$
14	16.60	1.50	1.48	$d_{33} = 1.45$ $d_{31} = 0.28$

two-dimensional charge-transfer molecules were also investigated by forming guest–host systems with PMMA. We found that all of these materials are SHG active in a poled guest–host system. The host molecules induce an alignment of guest molecules (dye) in a fashion that generates non-centrosymmetric crystal structures which leads to the appearance of an SHG signal. Table VII lists the refractive indices and NLO coefficients of dyes dispersed in a PMMA matrix. Two-dimensional charge-transfer molecules show d_{33} coefficient as high as 3.78 $pm\,V^{-1}$ for poled guest–host systems.

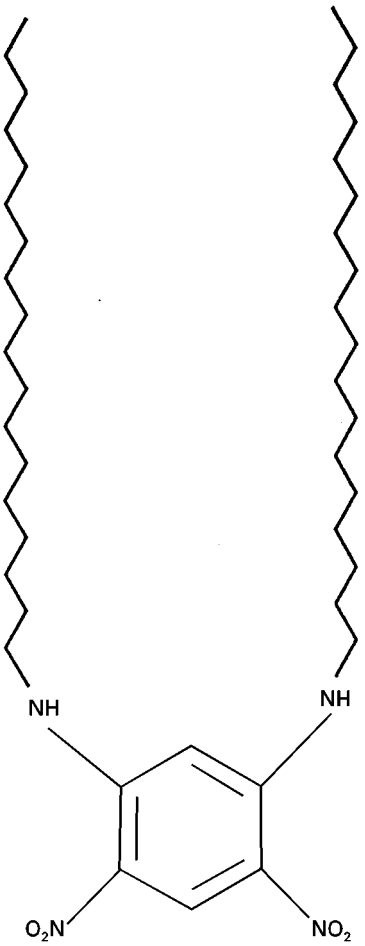

Figure 5 Chemical structure of the DIODD molecule (in the text).

3.3. Langmuir–Blodgett films

Fig. 5 shows the chemical structure of *N*,*N*′-dioctadecyl-2,4-dinitro-1,5-diaminobenzene (DIODD). A Miyata-type moving-wall LB trough (Nippon Laser Electronics, Japan) was used in this study. The surfactants used in film deposition were DIODD ($M_w = 703.10$), and arachidic acid ($M_w = 312.54$, Tokyo Kasei Co.). The surfactants of concentration of 10^{-3} M were spread from a chloroform solution on the deionized water surface containing 1×10^{-4} M $CdCl_2$ at 20 °C. The pH of the aqueous subphase was 6.0. The substrates used in film deposition were thoroughly cleaned glass slides which were made hydrophilic by the plasma technique. The alternate monolayers of a 1:1 mixture of DIODD with arachidic acid and pure arachidic acid were deposited at a surface pressure of 15 and 25 $mN\,m^{-1}$, respectively, by vertically dipping the substrate through the air–water interface at a rate of 5 $mm\,min^{-1}$ at 20 °C. The pressure–area isotherm (π–*A* curves) of a monolayer at the air–water interface was determined at a barrier speed of 20 $mm\,min^{-1}$. For SHG measurements, the LB monolayers were deposited on both sides of a fused silica substrate.

Fig. 6 shows the pressure–area isotherms for monolayers of pure DIODD, and 1:1 and 1:3 mixtures of DIODD and arachidic acid, respectively. Condensed DIODD monolayers containing Cd^{2+} ions can be formed at a surface pressure higher than 15 $mN\,m^{-1}$ but deposition of multilayers was not possible due to

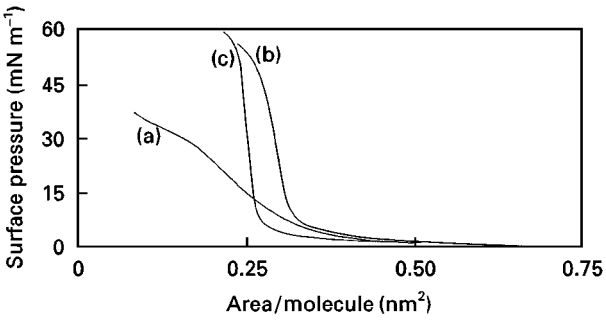

Figure 6 Pressure–area isotherms of monolayers of (a) pure DIODD; (b) 1:1 mixture and (c) 1:3 mixture of DIODD with arachidic acid, respectively. The solution spread with chloroform on deionized water subphase containing 10^{-4} M $CdCl_2$ at 20 °C. pH = 6.0, barrier spead = 20 $mm\,min^{-1}$, surface pressure 15 $mN\,m^{-1}$.

the instability of the monolayers. The monolayer of pure DIODD shows an expanded region (Fig. 6a). The surface area of a DIODD monolayer was estimated to be 0.49 nm^2/molecule from the space-filling model. Our DIODD molecule to some extent is somewhat similar to the LB molecules reported by Decher *et al.* [14] and Bubeck *et al.* [15]. Our results are in good agreement.

The LB films of pure DIODD were unstable, presumably because of the weak hydrophilic bonding of the electron-accepting nitro groups. Therefore, to

TABLE VIII Characteristics of Langmuir–Blodgett films of pure DIODD and its admixtures with arachidic acid (DIODD to arachidic ratio in the admixture)

Composition	Surface area (nm^2/molecule)	LB films features		
		Stability	X-ray diffraction	SHG
Pure DIODD	0.495	X	X	X
3:1	0.31	X	X	X
1:1	0.30	Moderate	Good	Yes
1:3	0.25	Good	Very good	X

X represents "None".

improve the stability of LB films, admixtures with the cadmium salt of arachidic acid were used. As expected, a 1:1 mixture of DIODD and arachidic acid forms a stable condensed monolayer (Fig. 6b) that has entirely different isotherm features compared with a pure DIODD monolayer. Interestingly, the LB films of 1:3 mixture of DIODD and arachidic acid were found to be even more stable and good in appearance (Fig. 6c). The formation of stable monolayers is assisted by the carboxylic group of arachidic acid because of increase in hydrophilicity. The monolayers of 1:1 as well as of 1:3 mixtures can be easily transferred from the LB trough on to a glass substrate. The monolayers of an 1:1 mixture show the limiting surface area of about 0.30 nm^2/molecule. Table VIII lists the characteristics of LB films of pure DIODD and on mixing with arachidic acid. Arachidic acid molecules are probably randomly arranged in the admixture LB monolayer. When compressed, the DIODD as well as arachidic acid molecules stand at the air–water interface and their long alkyl chains are oriented in the perpendicular direction to the air–water interface.

The refractive index of the LB films at different wavelengths was estimated by using the Sellmeier's equation. The refractive index of LB films does not change remarkably as a function of the incident angle. The ellipsometric measurements gave the following refractive index values of the DIODD LB monolayers:

$$n_\omega = 1.48 \text{ at } 1.064\,\mu m \quad \text{(fundamental wavelength, } \lambda\text{)}$$

$$n_{2\omega} = 1.57 \text{ at } 0.532\,\mu m \quad \text{(second-harmonic wavelength, } \lambda/2\text{)}.$$

The pure DIODD powder does not exhibit any SHG signal being centrosymmetric. Second-harmonic generation signals could be detected for a LB monolayer. Second-harmonic generation experiments performed at a wavelength of 1.064 μm show an SHG signal from the LB monolayer of a 1:1 mixture of DIODD and arachidic acid. The SHG signals are reproducible, and therefore are considered to originate from the DIODD LB monolayer. The SHG signals could only be detected for a 1:1 mixture, whereas neither 1:3 nor 3:1 mixtures showed any signal. It is rather difficult to explain why SHG was not observed for LB films containing arachidic acid and NLO chromophore at ratios of 1:3 and 3:1. A second-harmonic fringing pattern originates from dispersion of the refractive index of the substrate. This introduces a dephasing factor between harmonic waves generated at the front and back sides of the substrate [14, 15]. Second-order non-linear optical coefficients were calculated by fitting the fringing pattern according to a method developed by Kajzar and coworkers [30–32]. The SHG signals detected were calibrated against standard quartz ($d_{11} = 1.2 \times 10^{-9}$ esu) [33]. The second-order non-linear optical coefficient d_{11} of the monolayer corresponds to 11×10^{-9} esu. The d_{13} component is 3.85×10^{-9} esu, which is about one-third that of the d_{11} coefficient. From the following correlation

$$\chi^{(2)}_{IJK} = 2d_{IJK}(-2\omega; \omega, \omega) \quad (1)$$

the $\chi^{(2)}_{111}$ and $\chi^{(2)}_{133}$ values correspond to 22.0×10^{-9} and 6.70×10^{-9} esu, respectively. The second-order optical non-linear susceptibilities can be calculated theoretically from the molecular-oriented gas model [34].

$$d_{111} = N f_\omega f_\omega f_{2\omega} \bar{\beta}_{111}(-2\omega; \omega, \omega)\langle\cos^3\psi\rangle \quad (2)$$

where N is the number density of the molecule, f_ω and $f_{2\omega}$ are the local field factors, and the brackets denote averaging over the angle ψ. This equation represents a structural relationship between microscopic and macroscopic tensor which characterize the non-linearities of molecules having donor-acceptor interactions. The average molecular hyperpolarizability is related to the overall molecular orientation and its tensors can be expressed by [34]

$$\bar{\beta}_{IJK} = \sum \cos\theta_{Ii} \cos\theta_{Jj} \cos\theta_{Kk} \beta_{ijk} \quad (3)$$

where $\cos\theta_{Ii}$ are the scalar products $I \cdot i$ of unit vectors along film axis I and molecular axis i. We have derived the angular dependence of molecular hyperpolarizability β of the two-dimensional charge transfer molecules where components such as β_{xyy} must be considered because it is the largest β component contrary to one-dimensional charge transfer molecules in which β_{xxx} component is the largest. Here the x axis of the molecule is directed along a dipole moment and the y axis is perpendicular to the dipole moment within the molecular plane. We found that in two-dimensional charge-transfer molecules, the β_{xyy} component is always larger by a factor of three to five than that of the β_{xxx} component. To analyse the experimental data, we derived the following equations for the β components of two-dimensional charge-transfer molecules. The relationships X, Y, Z and x, y, z are written as follows, where x is the charge-transfer axis and the y axis is perpendicular to the charge-transfer axis and in the benzene ring. Where x of the molecule is inclined at an angle θ to the film normal, the y axis lies at some azimuthal angle, φ, with respect to the film axis 2 as shown in Fig. 7, and the azimuthal angles, φ, vary from one molecule to the other. The average molecular hyperpolarizability β in the film frame of reference is obtained by averaging over all molecular orientations, again using the standard transformation equations. Here, we assume that all azimuthal angles

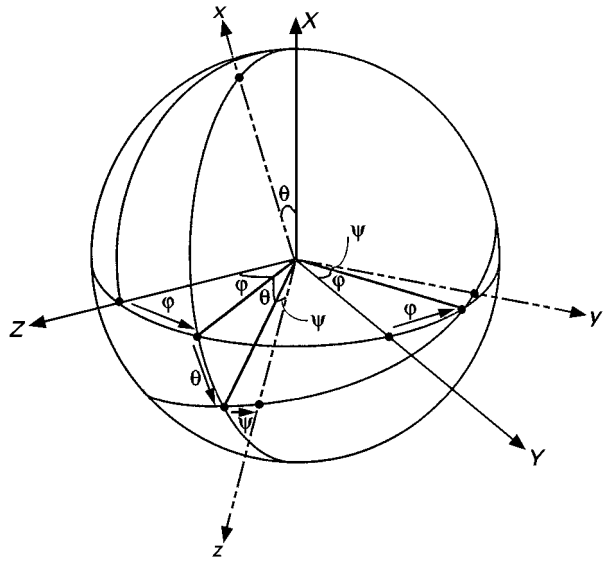

Figure 7 Coordinate axes for hyperpolarizability calculations defined for a two-dimensional charge-transfer molecular system. *X*, *Y* and *Z* are the LB film axes and *x*, *y*, and *z* are the molecular axes. θ defines the tilt angle to the film normal and φ defines the azimuthal angle which represents the angle between *Z* and the projection of *x* to the *Z*–*Y* plane.

are equally probable. Finally, $\bar{\beta}_{1\,1\,1}$ and $\bar{\beta}_{1\,3\,3}$ are represented by [26, 35, 36]

$$\bar{\beta}_{1\,1\,1} = \cos^3\theta\,\beta_{xxx} + 3\cos\theta\sin^2\theta\,\beta_{xyy} + 3\cos^2\theta\sin\theta\,\beta_{yxx} + \sin^3\theta\,\beta_{yyy} \quad (4)$$

$$\bar{\beta}_{1\,3\,3} = 0.5\cos\theta\sin^2\theta\beta_{xxx} + (0.5\cos^3\theta + \sin^2\theta\cos\theta)\,\beta_{xyy} + 0.5\cos\theta\,\beta_{xzz} + (\cos^2\theta\sin\theta + 0.5\sin^3\theta)\,\beta_{yxx} + 0.5\sin\theta\cos^2\theta\,\beta_{yyy} + 0.5\sin\theta\,\beta_{yzz} \quad (5)$$

Using these equations, average molecular hyperpolarizabilities $\beta_{1\,1\,1}$ and $\beta_{1\,3\,3}$ were calculated for the molecular tilt angle, θ, ranging from 0°–90°. To analyze the experimental data, we calculated the molecular hyperpolarizabilities, β, of a variety of model compounds of DIODD. The model compounds used in the study were 2,4-dinitro-1,5-diaminobenzene, *N*,*N*′-dimethyl-2,4-dinitro-1,5-diamino-benzene, and *N*,*N*′-diethyl-2,4-dinitro-1,5-diaminobenzene. In these molecules, electron-donating amino or alkylamino groups are located at *para* as well as *ortho*-positions to the electron accepting nitro groups, therefore dominantly *para* and *quasi-ortho* interactions lead to a two-dimentional charge-transfer character. Table V lists the molecular hyperpolarizability of model compounds having different alkyl chain lengths calculated by using the MOPAC AM1 method [20]. The β value increases as the number of carbon atoms increases in the alkyl chain and reaches values even higher than the β values of the *p*-nitroaniline molecule. In addition, like one-dimensional charge-transfer molecules, the molecular hyperpolarizabilities of two-dimensional charge-transfer molecules can be increased remarkably by introducing long π-conjugation in the molecules, for example by incorporating stilbene, azobenzene, and benzylidene units and as a result large second-order optical non-linearities can be obtained by applying the molecular designing approach [26]. In the case of alkyl chains, the enhancement of molecular hyperpolarizability for the dialkylamino group is saturated when the alkyl chain exceeds a certain length [37, 38] and a similar trend has been observed in the results from our theoretical calculations. Therefore, *N*,*N*′-diethyl-2,4-dinitro-1,5-diaminobenzene was used as a model compound for the DIODD. The average hyperpolarizabilities $\beta_{1\,1\,1}$ and $\beta_{1\,3\,3}$ of the model compound calculated by the Molecular Orbital Package (MOPAC) AM1 were 15.2×10^{-30} and 5.3×10^{-30} esu, respectively, at a tilt angle of 60°. Theoretical calculations of second-order optical non-linear susceptibilities were performed by using a molecular-oriented gas model in Equation 7. The second-order optical non-linearities were calculated theoretically for the DIODD, where *N*, the number of molecules per unit volume is 5.9×10^{20} mol cm^{-3} and f_w and f_{2w}, the local field factors at the fundamental and harmonic, correspond to 1.951 and 1.488, respectively. The calculated d_{11} and d_{13} components are 26.0×10^{-9} ($\chi^{(2)}_{1\,1\,1} = 52.0 \times 10^{-9}$ esu) and 9.15×10^{-9} esu, ($\chi^{(2)}_{1\,3\,3} = 18.3 \times 10^{-9}$ esu), respectively and have a ratio 1 : 0.34, very similar to our experimental results. By using these data, molecular hyperpolarizability can be calculated as a function of tilt angle according to Equations 4 and 5. The microscopic molecular hyperpolarizability is strongly affected by the variation of the molecular tilt angle, ϕ, as shown in Fig. 8. The molecular hyperpolarizability shows a maxima at an angle of 56°. In the case of one-dimensional charge-transfer molecules, for optimizing the $\chi^{(2)}_{1\,1\,1}$ component, a polar molecule must align normal to the substrate (i.e. at an angle of 90°), otherwise the magnitude of $\chi^{(2)}_{1\,1\,1}$ decreases from the maximum value. On the other hand, the situation is entirely different for the two-dimensional charge-transfer molecule, even if the molecule is inclined from the normal to the substrate, the large $\chi^{(2)}_{1\,1\,1}$ could be obtained. Interestingly, the maximum d_{11} and d_{13} values of 26.5×10^{-9} esu ($\chi^{(2)}_{1\,1\,1} = 53 \times 10^{-9}$ esu) and 10×10^{-9} esu ($\chi^{(2)}_{1\,3\,3} = 20 \times 10^{-9}$ esu), respectively, are obtained at a tilt angle of 56°. By fitting the ratio between $\beta_{1\,1\,1}$ and $\beta_{1\,3\,3}$ obtained from the experimental data to the theoretical values, the tilt angle of the charge-transfer axis of an LB molecule can be estimated. Our results demonstrate that the average tilt angle between the charge-transfer axis of the DIODD molecule and the normal to the substrate is about 60°. The magnitude of theoretically calculated second-order optical non-linearities is in good agreement with the experimental results, which also confirms the validity of Equations 4 and 5. The tilt angle differs only by 4° indicating that the orientation of the DIODD molecules on the substrate is very close to the desired optimal molecular orientation. Therefore, our experimental and theoretical data analysis provides a basis for the best molecular orientation

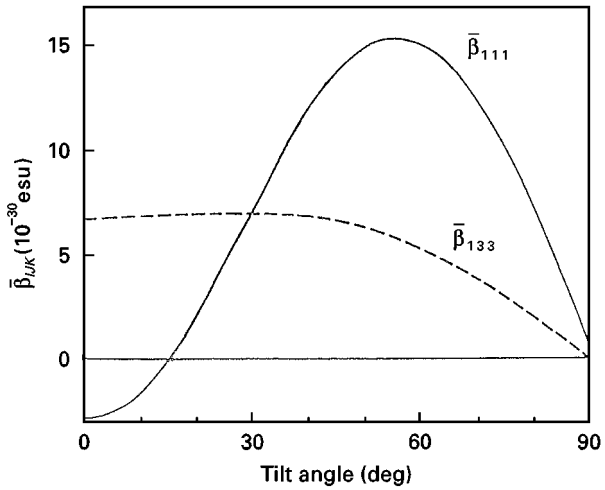

Figure 8 Molecular tilt-angle dependence of the molecular hyperpolarizabilities ($\bar{\beta}_{111}$ and $\bar{\beta}_{133}$) for a two-dimensional charge-transfer molecule showing a relationship between second-order optical non-linearity and molecular orientation.

of a two-dimensional charge-transfer molecule for optimizing second-order optical non-linearity in LB monolayers.

The LB monolayers of amphiphilic phenylhydrazone and styrylpyridinium compounds exhibit $\chi^{(2)}_{111}$ in the range of $9.0–350 \times 10^{-9}$ esu, depending upon the nature of the different functional groups [15]. The $\chi^{(2)}_{111}$ and $\chi^{(2)}_{133}$ of pure 2-docosylamino-5-nitropyridine as 3.2×10^{-9} and 4.28×10^{-9} esu, respectively, have been reported [14]. The magnitude of the non-linear optical coefficients of DIODD falls within the range of the highly conjugated phenylhydrazone compounds recently reported by Bubeck *et al.* [15] taking into account the density of DIODD molecules. In a 1:1 mixture of DIODD with arachidic acid, the dilution of the chromophore leads to rather smaller non-linear optical coefficients. The DIODD molecule shows a cut-off wavelength of 470 nm, which is far from the resonant region, therefore, our $\chi^{(2)}$ values are a purely non-resonant parameter. The β value of the DIODD molecule is about three orders of magnitude smaller than that of styrylpyridinium salts and phenylhydrazone dyes as a consequence, a relatively smaller second-order non-linear susceptibility $\chi^{(2)}$ can be anticipated compared to the long π-conjugated charge-transfer LB molecules. Therefore, the $\chi^{(2)}$ values of the DIODD molecule are reasonably large. Other two-dimensional charge-transfer molecules consisting of long π-conjugated systems show much larger molecular hyperpolarizabilities. For example, a two-dimensional charge-transfer molecule 1,3-diamino-4,6-*bis*(2,4′-dinitrophenyl)benzene shows very large $\beta_{xxx} = -9.40 \times 10^{-30}$ and $\beta_{xyy} = -47.36 \times 10^{-30}$ esu as reported by Watanabe *et al.* [18]. The non-linear optical properties of two-dimensional charge-transfer molecules which possess large off-diagonal β component on mixing with conventional polymer matrices show little decay after the dipolar orientation relaxation. Therefore, two-dimensional charge-transfer molecules possessing off-diagonal β components are a new class of non-linear optical materials for LB films as well as for non-linear poled polymers. In a recent study by the authors, when an octadecylamino chain in the DIODD molecule was substituted by a fluorine atom, the new amphiphile *N*-octadecyl-2,4-dinitro-5-fluoroaniline (ODDFA) attains an one-dimensional charge-transfer character [24]. The ODDFA itself forms stable monolayers on the water surface and their monolayers can be easily transferred on to a solid substrate. The Langmuir–Blodgett monolayer of pure ODDFA exhibits d_{11} and d_{13} coefficients of 19×10^{-9} and 6.7×10^{-9} esu, respectively, at a tilt angle of 40°. Therefore, this chemical modification assists in designing suitable molecules for Langmuir–Blodgett films.

The structural features of the LB molecules indicate that the bulky alkyl chain molecules tend to incline from the normal axis of the substrate. While using one-dimensional charge-transfer LB molecules to optimize optical non-linearity, polar molecules must align normal to the substrate (at an angle of 90°), otherwise the magnitude of optical non-linearity decreases from the maximum. On the other hand, in the case of two-dimensional charge-transfer molecules, if the LB molecules incline from the normal axis of the substrate, large second-order non-linear optical coefficients can be obtained. Therefore, these results indicate a new direction in the molecular design of LB mono- and multilayers for obtaining large second-order optical non-linearities utilizing off-diagonal b component.

4. Conclusion

This comparative study of *N*,*N*′-dialkyl-4,6-dintro-1,3-diaminobenzenes has demonstrated that the alkyl chain length plays a major role in determining physical properties. The ^{13}C-NMR spectroscopy technique assists in assigning the carbons of alkyl chain lengths up to C_8H_{17} in *N*,*N*′-dialkyl-2,4-dinitro-1,5-diaminobenzenes and up to $C_{10}H_{21}$ in *N*-alkyl-4,6-dinitro-3-halo-diaminobenzenes. The experimental NMR data are in good agreement with empirical calculations. Two-dimensional charge-transfer molecules offer a new direction in the molecular design of novel materials for non-linear optics.

Two-dimensional charge-transfer molecules form an important class of organic non-linear optical materials for second-harmonic generation. The molecular hyperpolarizability, β, of two-dimensional charge-transfer molecules is of the same magnitude as of one-dimensional charge-transfer molecules most commonly considered for applications in non-linear optics. Our studies show for the first time that large second-order optical non-linearities $\chi^{(2)}(-2\omega; \omega, \omega)$ can be achieved in two-dimensional charge-transfer LB films at a tilt angle of about 56°, and in such cases, they seem more effective than that of one-dimensional charge-transfer molecules. One of the advantages offered by the two-dimensional charge-transfer molecules over one-dimensional charge-transfer LB molecules is their ability to maintain optimum second-order non-linear susceptibility even if they are inclined

from normal to the substrate. The molecular hyperpolarizability, β, value increases as the number of carbon atoms increases in the alkyl chain, and reaches even higher than the β values of the standard one-dimensional charge-transfer molecule of *p*-nitroaniline. In addition, the molecular hyperpolarizabilities of two-dimensional charge-transfer molecules can be further increased by introducing longer π-conjugation such as stilbene, azobenzene, and benzylidene units and, as a result, significantly large second-order optical non-linearities $\chi^{(2)}(-2\omega; \omega, \omega)$ can be obtained. Studies of other analogous two-dimensional charge-transfer molecules of interest would further stimulate research in this field and it should not be long before the potential applications of this novel class of nonlinear optical materials will be realized.

References

1. D. S. CHEMLA and J. ZYSS (eds), "Nonlinear Optical Properties of Organic Molecules and Crystals", Vol. I–II, (Academic Press, New York, 1987).
2. J. ZYSS (ed.), "Molecular Nonlinear Optics" (Academic Press, New York, 1994).
3. H. S. NALWA and S. MIYATA (eds), "Nonlinear Optics of Organic Molecules and Polymers" (CRC Press, Boca Raton, FL, 1997).
4. H. S. NALWA, T. WATANABE and S. MIYATA, in "Progress in Photochemistry and Photophysics", Vol. V, edited by J. F. Rabek (CRC Press, Boca Raton, FL, 1992) Ch. 4 pp. 103–485.
5. *Idem*., in "Nonlinear Optics of Organic Molecules and Polymers", edited by H. S. Nalwa and S. Miyata (CRC Press, Boca Raton, FL, 1997) Ch. 4, pp. 89–350.
6. H. S. NALWA and J. S. SHIRK, in "Phthalocyanines: Properties and Applications", Vol. 4, edited by C. C. Leznoff and A. B. P. Lever (VCH, New York, 1996) Ch. 3, pp. 79–181.
7. H. S. NALWA, in "Nonlinear Optics of Organic Molecules and Polymers", edited by H. S. Nalwa and S. Miyata (CRC Press, Boca Raton, FL, 1997) Ch. 11, pp. 611–797.
8. *Idem*., *Adv. Mater*. **5** (1993) 341.
9. *Idem*., *Appl. Organomet. Chem*., **5** (1991) 349.
10. S. MIYATA, T. WATANABE and H. S. NALWA, in Proceedings of the International School of Physics "Enrico Fermi", "Nonlinear Optical Materials: Principles and Applications", edited by V. Degiorgio and C. Flytzanis (IOS Press, Amsterdam, 1995) p. 225.
11. J. ZYSS, N. F. NICOUD and M. COQUILLAY, *J. Chem. Phys*. **81** (1984) 4160.
12. H. S. NALWA and A. KAKUTA, *Appl. Organometal. Chem*. **6** (1992) 645.
13. I. R. GIRLING, P. V. KOLINSKY, N. A. CADE, J. D. EARLS and I. R. PETERSON, *Opt. Commun*., **35** (1985) 289.
14. G. DECHER, B. TIEKE, C. BOSSHARD and P. GUNTER, *Ferroelectrics* **91** (1989) 193.
15. C. BUBECK, A. LASCHEWSKY, D. LUPO, D. NEHER, P. OTTENBREIT, W. PAULUS, W. PRASS, H. RINGSDORT and G. WEGNER, *Adv. Mater*. **3** (1991) 54.
16. F. KAJZAR, J. MESSIER, J. ZYSS, and I. LEDOUX, *Opt. Commun*. **45** (1983) 133.
17. D. LUPO, W. PRASS, U. SCHEUNEMANN, A. LASCHEWSKY, H. RINGSDORF and I. LEDOUX, *J. Opt. Soc. Am. B* **5** (1988) 300.
18. T. WATANABE, M. KAGAMI, H. MIYAMOTO, A. KIDOGUCHI and S. MIYATA, in "Nonlinear Optics", edited by S. Miyata (Elsevier, Amsterdam, 1992) p. 201.
19. H. S. NALWA, T. WATANABE, K. NAKAJIMA and S. MIYATA, *ibid*., p. 271.
20. M. J. S. DEWAR, E. G. ZOEBISCH, E. F. HEALY and J. P. S. STEWART, *J. Am. Chem. Soc*. **107** (1985) 3902.
21. H. KALINOWSKI, S. BERGER and S. BRAUN, "Carbon-13 NMR Spectroscopy" (Wiley, New York, 1988).
22. L. P. LINDEMAN and J. Q. ADAMS, *Anal. Chem*. **43** (1971) 1245.
23. G. B. SATITSKY and K. NAMIKAWA, *J. Phys. Chem*. **67** (1961) 731.
24. H. S. NALWA, T. WATANABE, K. NAKAJIMA and S. MIYATA, *Thin Solid Films* **227** (1993) 205.
25. L. T. CHENG, W. TAM, S. H. STEVENSON, G. R. MEREDITH, G. RIKKEN and S. R. MARDER, *J. Phys. Chem*. **95** (1991) 10631
26. T. KONDO, N. OGASAWARA, S. UMEGAKI and R. ITO, *SPIE Proc*. **971** (1988) 83.
27. H. S. NALWA, T. WATANABE and S. MIYATA, *Adv. Mater*. **7** (1995) 1001.
28. N. OKAMOTO, T. ABE, D. CHEN, H. FUJIMURA and R. MATSUSHIMA, *Opt. Commun*. **74** (1990) 421.
29. S. TASAKA, T. ABE, R. MATSUSHIMA, M. SUZUKI, D. CHEN and N. OKAMOTO, *Jpn Appl. Phys*. **30** (1991) 296.
30. F. KAJZAR and J. MESSIER, *Phys. Rev. A* **52** (1985) 2352.
31. *Idem*., *Thin Solid Films* **132** (1985) 11.
32. F. KAJZAR and I. LEDOUX, *ibid*. **179** (1989) 359.
33. M. CHOY and R. L. BYER, *Phys. Rev. B* **14** (1976) 1693.
34. J. L. OUDAR and J. ZYSS, *Phys. Rev. A* **26** (1982) 2016.
35. H. S. NALWA, K. NAKAJIMA, T. WATANABE, K. NAKAMURA, A. YAMADA and S. MIYATA, *Jpn J. Appl. Phys*. **30** (1991) 983.
36. T. WATANABE, X. T. TAO, J. KIM, S. MIYATA, H. S. NALWA and S. C. LEE, *Non-linear Optics* **15** (1996) 327.
37. G. BERKOVIC, Th. RASING and Y. R. SHEN, *J. Opt. Soc. Am. B*. **4** (1987) 945.
38. Th. RASING, G. BERKOVIC, Y. R. SHEN, S. G. GRUBB and M. W. KIM, *Chem. Phys. Lett*. **130** (1986) 1.

Received 30 July 1996
and accepted 22 April 1998